Hindawi
Journal of Nanomaterials
Volume 2022, Article ID 2558419, 12 pages
https://doi.org/10.1155/2022/2558419

Research Article

Impact of Ferromagnetic Nanoparticles Submerged in Chemically Reactive Viscoelastic Fluid Transport Influenced by Double Magnetic Dipole

N. Kousar,[1] **Taher A. Nofal**,[2] **W. Tahir**,[1] **S. M. Bilal**,[1] **and Ndolane Sene**[3]

[1]*Department of Mathematics, Air University, E-9 Islamabad 44000, Pakistan*
[2]*Department of Mathematics and Statistics, College of Science, Taif University, P.O. Box 11099, Taif 21944, Saudi Arabia*
[3]*Laboratoire Lmdan, Departement De Mathematiques De Decision, FacultÌe Des Sciences Economiques Et Gestion, Universite Cheikh Anta Diop De Dakar, BP 5683 Dakar Fann, Senegal*

Correspondence should be addressed to Ndolane Sene; ndolanesene@yahoo.fr

Received 13 January 2022; Revised 20 February 2022; Accepted 1 March 2022; Published 1 April 2022

Academic Editor: Taza Gul

The present article summarized the effects of double magnetic dipole for chemically reactive viscoelastic fluid in the presence of two different ferromagnetic particles, namely, nickel zinc ferrite $(NiZnFe_2O_4)$ and magnetite ferrite (Fe_3O_4). Due to double magnetic dipole, an external magnetic field is applied normal to the flow. Blood is used as base fluid due to its viscoelastic fluid properties. The Cattaneo-Christov heat flux model is used for heat transport phenomena. The physical model is formulated in the form of partial differential equations which are then converted into ordinary differential equations using the suitable transformations. The system is solved numerically using shooting method along with Runge-Kutta-Fehlberg method. The characteristics of different parameters like the strength of homogeneous-heterogeneous reactions (k_1 and k_2), ferrohydrodynamic interaction (β_1), Schmidt number (S_c), Deborah number (α_{1a}), and thermal relaxation time (α_{1c}) on velocity, temperature, and concentration profiles are analyzed through graphs and in tabular form. It has been observed that as magnetic dipole creates a force which attracts the ferrite particles, hence, it slows down the velocity profile. Concentration field depresses due to the presence of strength of heterogeneous reaction parameter k_2.It is also noted that by expanding values of thermal relaxation time (α_{1c}), the temperature profile shows a reverse behavior.

1. Introduction

Ferrofluids lie in the category of smart materials those consist of micron-sized colloidal magnetic nanoparticles that are saturated in a nonmagnetic base fluid. The most fascinating feature of these fluids is its highly magnetizing ability when an external magnetic field is applied. Pappell [1] initially highlighted the characteristic of ferrofluid in 1963. He utilized ferrofluid in a weightless atmosphere in terms of liquid rocket fuel, which is pinched near a pump inlet by applying an external magnetic field. Ferrofluids have many appealing applications in electrical instruments such as in hard disk, rotating X-ray tubes, shafts, and rods. The role of ferrofluids in biomedical equipment's is no doubt incredible, which is helpful in the process of wound treatment, asthma treatment, removal of cancer with hyperthermia, and many more. For these kinds of procedures, the homogeneous and heterogeneous have great importance. The homogenous and heterogeneous reactions take places in the bulk and occur on the catalyst surface, respectively. Whether the process is homogeneous or heterogeneous depends upon the situation that they exist in the absolute majority of the fluid or a part of catalytic surfaces. In essence, the homogeneous process is continuously intact within the given phase, whereas heterogeneous reactions have restricted boundaries. There are also a variety of chemically reacting structures that involve both h-h reactions termed as such as catalysis, burning, and biochemical reacting systems. In this flow, due to an external flow applied on the outer region of boundary layer, there exists a reaction in

that region as explained by [2, 3]. Initially, Andersson and Valnes [4] studied the viscous ferrofluid with magnetic dipole effects on the stretching surface. They examined the influence of magnetothermomechanical coupling on the fluid. Numerical studies related to ferrofluid inside a channel with cold walls focusing on a line source dipole delineated by Ganguly et al. [5]. In a porous medium, Sharma et al. [6] specified the attributes of convection by focusing dust particles on a ferromagnetic fluid. The results corresponding to characteristics of heat transfer in a Darcy number ferrofluid flow with porous wall is analyzed by Strek [7]. The dipole effects in a ferrofluid flow origin below the channel with isothermal wall were studied by Strek and Jopek [8]. They focused on time dependent heat transfer and analyzed the spatial alteration creating magnetization because of gradient effects, depending temperature magnetic susceptibility for ferrofluids. Sadiq et al. [9] studied the Casson fluid model to study the thermal performance under the Brownian and thermoheretic effects of hybrid nanoparticles. The dipole's magnetization in the series flow of ferrofluid taking elongated surface highlighting thermal radiation is explored by Makinde and Aziz [10]. Aminfar et al. [11] implement a non-acting magnetic field inside a vertical tube during the numerical studies of mixed convection of ferrofluid. During his studies, he used both + and - types of magnetic gradients; the (-) gradient of magnetic field reacts the same as the buoyancy forces and boosts the Nusselt number, whereas the magnetic field with a (+) gradient decelerates it. A stagnation point flow along elongated sheet in the presence of heterogeneous-homogeneous reactions that is analyzed by Bachok et al. [12] analyzed a chemically reactive stagnation point flow over the elongated sheet. In his paper, he discussed the case of fluid having less kinetic viscosity in which he observed that when the extending velocity is low as compared to free steam velocity, a boundary layer is achieved, whereas the inverted boundary layer attains in the case when stretching the velocity exceeds the free steam velocity. Affixing 2-phase mixture model and effecting control volume method, Aminfar et al. [13] executed the transversal non acting magnetic field accomplishing electric current during the inspection of flowing ferrofluid inside a duct. They showed the flourishing behavior of average heat transfer coefficient. The shrinking surface is taken by Kameswaran et al. [14] during the investigation of homogeneous-heterogeneous reaction in a porous medium. By taking into account the radiation effect in an extended sheet, Titus and Abraham [15] used ferrofluid. It also concludes that due to magnetic field local vortex vary the advection energy transport also boosting heat transfer ability. Sheikholeslami et al. [16] conferred the aspects of non-uniform magneto hydrodynamic flow of ferroliquid utilizing convective heat transport. Hayat et al. [17] also detailed the effects of MHD nanofluid with heterogeneous-homogeneous reaction and velocity slip condition. It is concluded that in the case of concentration, both homogeneous and heterogeneous parameters show a reverse behavior. Imtiaz et al. [18] reflected the impact of homogeneous and heterogeneous reactions in the examination of MHD flow in a curved stretchable surface. He depicted the increasing behavior between curvature parameter and fluid velocity. Due to many applications, the boundary layer flow of non-Newtonian fluids with different effects has added an enormous attraction in the recent years [19–33].

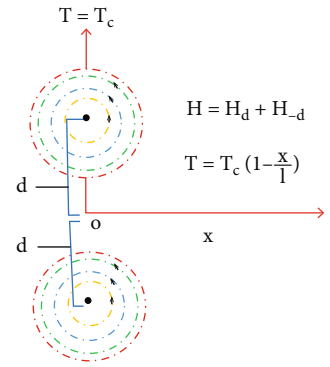

Figure 1: Geometry of flow model.

The ultimate goal of this research is to scrutinize the effects of magnetic double dipole in the examination of Maxwell ferrofluid which is composed of base fluid blood, whereas ferrite particles were used as $(NiZnFe_2O_4$ and $Fe_3O_4)$ under the high lightening impact of homogenous and heterogeneous reaction. Also, the concentration levels of these particles are about 20% into the base fluid. The basic theme of including these ferrite particles is to enhance the strength of heat transferring phenomena which is the inspiration of this research. Brief literature survey is summarized in Section 1. Section 2 is focused on the mathematical formulation of problem. In Section 3, the computational procedure is discussed in details. The possible outcomes of the current study are deliberated in Section 4. Section 5 presents the key features of this article.

2. Mathematical Formulation

Consider a steady 2D flow of an incompressible non-Newtonian Maxwell electrically conducting a ferromagnetic fluid running on a flat surface in x direction as shown in Figure 1. The location of dipole is set in the$y$direction as the displacement between the dipole and surface is taken as$d$, while the magnetic field(H)generated with the presence of magnetic dipole directions as$x$ -axis. The scalar potential of permanent magnetic dipole which influences ferrofluid defined in [2] is

$$\delta_a = -\frac{I_0}{2\pi}\left[\mathrm{Tan}^{-1}\left(\frac{y+d}{x}\right) + \mathrm{Tan}^{-1}\left(\frac{y+d}{x}\right)\right], \quad (1)$$

where I_0 is the representation of dipole moment per unit length. The relation between gradient of magnetic scalar potential δ_a and applied magnetic field is held as $H_1 = -\nabla$

δ_a. The components of H_1 are

$$H_x = -\frac{\partial \delta_a}{\partial x} = -\frac{I_0}{2\pi}\left[\frac{y+d}{x^2+(y+d)^2} + \frac{y-d}{x^2+(y-d)^2}\right],$$
$$H_y = -\frac{\partial \delta_a}{\partial y} = -\frac{I_0}{2\pi}\left[\frac{x}{x^2+(y-d)^2} + \frac{x}{x^2+(y+d)^2}\right]. \quad (2)$$

The force field strength has a resultant magnitude H, with their element forms that are termed as

$$H = \left[\left(\frac{\partial \delta_a}{\partial x}\right)^2 + \left(\frac{\partial \delta_a}{\partial y}\right)^2\right]^{\frac{1}{2}}, \quad (3)$$

$$(\nabla H)_x = \frac{\partial \delta_a/\partial x\left(\partial^2 \delta_a/\partial x^2\right) + \left(\partial \delta_a/\partial y\right)\left(\partial^2 \delta_a/\partial x \partial y\right)}{\left[\left(\partial \delta_a/\partial x\right)^2 + \left(\partial \delta_a/\partial y\right)^2\right]^{1/2}}, \quad (4)$$

$$(\nabla H)_y = \frac{\partial \delta_a/\partial x\left(\partial^2 \delta_a/\partial x \partial y\right) + \left(\partial \delta_a/\partial y\right)\left(\partial^2 \delta_a/\partial y^2\right)}{\left[\left(\partial \delta_a/\partial x\right)^2 + \left(\partial \delta_a/\partial y\right)^2\right]^{1/2}}. \quad (5)$$

Experiencing Equation (1) in Equations (4)-(5), we get the following form by expanding up to order x^2:

$$(\nabla H)_y = 0. \quad (6)$$

The assuming effects of surface's wall is $(\partial \delta_a/\partial x)_{y=0} = (\partial^2 \delta_a/\partial y^2)_{y=0} = 0$, with including assumption that $x \gg$ d We get the transformed form of equation (4)

$$(\nabla H)_x = -\frac{I_0}{\pi}\frac{1}{x^2}. \quad (7)$$

The change in magnetization M can be expressed as

$$M = \mathrm{K}_1(\mathrm{T}_c\text{-T}). \quad (8)$$

2.1. Analysis of Flow. We have considered a viscoelastic fluid flow over a flat surface with double magnetic dipoles, which are placing at a space (d) from the wall and perpendicular to the surface. Consider l as the length of plate (l>>d) with the wall. The temperature changes linearly with the plate length that is defined as $T_w = T_c(1 - x/l)$. In the boundary layer flow, the connection between homogeneous and heterogeneous reactions adding 2-species chemically, named, A and B, are taken following Chaudhary and Merkin [2] as

$$A + 2\mathrm{B} \longrightarrow 3\mathrm{B}, \text{ rate} = \mathrm{k}_c a b^2.$$
$$A \longrightarrow \mathrm{B}, \text{ rate} = \mathrm{k}_s a \quad (9)$$

Concentrations A and B are represented by a and b, and k_i (i = c, s) are termed as rate constants. The process is considered to be isothermal for both reactions.

The corresponding flow equations in the presence of magnetic dipole are

$$\frac{\partial u}{\partial x} + \frac{\partial v}{\partial y} = 0,$$
$$\left(u\frac{\partial u}{\partial x} + v\frac{\partial u}{\partial y}\right) + \lambda_a\left(u^2\frac{\partial^2 u}{\partial x^2} + v^2\frac{\partial^2 u}{\partial y^2} + 2uv\right) = \frac{\mu_0}{\rho_{nf}}M\frac{\partial H}{\partial x} + \frac{\mu_{nf}}{\rho_{nf}}\frac{\partial^2 u}{\partial y^2},$$
$$\left(u\frac{\partial T}{\partial x} + v\frac{\partial T}{\partial y}\right) + \lambda_c\left(u\frac{\partial u}{\partial x}\frac{\partial T}{\partial x} + v\frac{\partial v}{\partial y}\frac{\partial T}{\partial y} + u\frac{\partial v}{\partial x}\frac{\partial T}{\partial y} + v\frac{\partial u}{\partial y}\frac{\partial T}{\partial x} + 2uv\frac{\partial^2 T}{\partial x \partial y} + u^2\frac{\partial^2 T}{\partial x^2} + v^2\frac{\partial T^2}{\partial y^2}\right) = \frac{k_{nf}}{(\rho c_p)_{nf}}\frac{\partial^2 T}{\partial y^2}, \quad (10)$$
$$\mathrm{u}\frac{\partial a}{\partial x} + \mathrm{v}\frac{\partial a}{\partial y} = \mathrm{D}_A\frac{\partial^2 a}{\partial y^2} - \mathrm{k}_c a \mathrm{b}^2,$$
$$\mathrm{u}\frac{\partial b}{\partial x} + \mathrm{v}\frac{\partial b}{\partial y} = \mathrm{D}_B\frac{\partial^2 a}{\partial y^2} + \mathrm{k}_c a \mathrm{b}^2.$$

The admissible flow conditions are

$$u|_{y=0} = 0, v|_{y=0} = 0, T|_{y=0} = T_c\left(1 - \frac{x}{l}\right), \mathrm{D}_A\frac{\partial a}{\partial y}\Big|_{y\longrightarrow 0} = \mathrm{k}_s \mathrm{a}(0), \mathrm{D}_B\frac{\partial a}{\partial y}\Big|_{y\longrightarrow 0}$$
$$= -\mathrm{k}_s \mathrm{a}(0),$$
$$u|_{y\longrightarrow\infty} = \mathrm{u}_0, T|_{y\longrightarrow\infty} = T_c, a|_{y\longrightarrow\infty} \longrightarrow \mathrm{a}_0, \mathrm{b}|_{y\longrightarrow\infty} \longrightarrow 0. \quad (11)$$

where (u,v) is the velocity components along x and y directions, (μ_0) is the magnetic permeability, (μ_{nf}) is the dynamic viscosity, (ν_{nf}) is the kinematic viscosity of nanofluid, (ρ_{nf}) is the nanofluid density, $(\rho c_p)_{nf}$ is the specific heat, (k_{nf}) represented as thermal conductivity of the nanofluid, (λ_a) is the relaxation time of fluid, and (λ_c) identifies as the relaxation time of heat flux.

Table 1: Thermophysical properties of blood, nickel zinc ferrite, and magnetite ferrite.

	$\rho(\mathrm{kg/m^3})$	C_p(J/kgK)	k(W/mK)
Blood	1060.0	3770	0.52
Nickel zinc ferrite	4800	710	6.3
Magnetite ferrite	5180	670	9.7

Table 2: Grid independence for Nusselt number and skin friction for $\beta = 0.1, \lambda = 0.01, \gamma = 1.0, \mathrm{Pr} = 6.0$..

ζ	Nusselt number	Skin friction
$\mathbf{10^{-2}}$	3.9475	2.5523
$\mathbf{10^{-4}}$	3.9471	2.5514
$\mathbf{10^{-6}}$	3.9471	2.5514

2.2. Thermophysical Properties. Using similarity transform as defined by [23],

$$\eta = \left(\frac{u_0}{vx}\right)^{\frac{1}{2}} y,\ T = T_c\left(1 - \frac{x}{l}\theta(\eta)\right),$$
$$u = u_0 f'(\eta),\ v = \left(\frac{vu_0}{x}\right)^{\frac{1}{2}}\left(\frac{\eta f'(\eta)}{2} - \frac{f(\eta)}{2}\right), \tag{12}$$
$$a = a_0\, g(\eta),\ b = a_0\, h(\eta).$$

By implementing similarity variables express in Eq. (12), our modified equations take the subsequent form:

$$\left(\frac{1}{(1-\phi)^{2.5}\left(1-\phi+\phi\left(\rho_s/\rho_f\right)\right)} - \frac{\alpha_{1a} f^2}{4}\right) f''' + \frac{ff''}{2} - \frac{\alpha_{1a}}{4}\left(f'^2 f''\eta + 2ff' f''\right) - \frac{\beta_1\theta}{\left(1-\phi+\phi\left(\rho_s/\rho_f\right)\right)} = 0, \tag{13}$$

$$\left(\frac{k_{nf}/k_f}{\left(1-\phi+\phi\left(\left(\rho C_p\right)_s/\left(\rho C_p\right)_f\right)\right)} - \frac{\alpha_{1c}\,\mathrm{Pr}\, f^2}{4}\right)\theta_1'' + \mathrm{Pr}\left(\frac{f\theta'}{2} - f'\theta + \frac{\alpha_{1c}}{4}\left(2ff'' + 2ff'\theta'\right)\right) = 0, \tag{14}$$

$$\frac{1}{S_c} g'' + fg' - k_1 gh^2 = 0, \tag{15}$$

$$\frac{\delta}{S_c} h'' + fh' + k_1 gh^2 = 0, \tag{16}$$

with nondimensional boundary conditions:

$$f(\eta) = f'(\eta) = 0, \theta(\eta) = 1, g'(\eta) = k_2\, g(\eta), \delta h'(\eta) = -k_2 g(\eta) \text{ at } \eta = 0,$$
$$f'(\eta) \longrightarrow 1, \theta(\eta) \longrightarrow 0, g(\eta) = 1, h(\eta) = 0 \text{ as } \eta \longrightarrow \infty. \tag{17}$$

Table 3: Obtained values of $-\boldsymbol{\theta'(0)}$ by altering values of β and Pr.

$\boldsymbol{\beta}$	$\boldsymbol{Pr}$	$-\boldsymbol{\theta'(0)}$
$(\boldsymbol{NiZnFe_2O_4})$		
0.0		3.0554
1.0	5	3.0180
2.0		3.0074
	4	3.0000
1.0	5	3.0180
	6	3.1079
$(\boldsymbol{Fe_3O_4})$		
0.0		3.0904
1.0	5	3.0489
2.0		3.0093
	4	3.0060
1.0	5	3.0489
	6	3.1479

Table 4: Obtained values of $g'(0)$ by altering values of k_1, k_2 and S_c .

$\boldsymbol{k_1}$	$\boldsymbol{k_2}$	$\boldsymbol{S_c}$	$\boldsymbol{g'(0)}$
$(\boldsymbol{NiZnFe_2O_4})$			
0.1			1.3726
0.3		0.1	1.3931
0.5			1.4145
		0.1	1.3726
0.1		0.2	1.1121
		0.3	0.8977
	0.1		1.3726
	0.3	0.1	2.0805
	0.5		2.5090
		0.1	1.3726
	0.1	0.2	1.1121
		0.3	0.8977
$(\boldsymbol{Fe_3O_4})$			
0.1			1.2858
0.3		0.1	1.3051
0.5			1.3253
		0.1	1.2858
0.1		0.2	1.0510
		0.3	0.8555
	0.1		1.2858
	0.3	0.1	1.9481
	0.5		2.3486
		0.1	1.2858
	0.1	0.2	1.0510
		0.3	0.8555

In Eqs. (13)-(16), β_1 is the ferrohydrodynamic interaction, Pr defines the Prandtl number, α_{1a} mean the Deborah number, α_{1c} is represented here as a

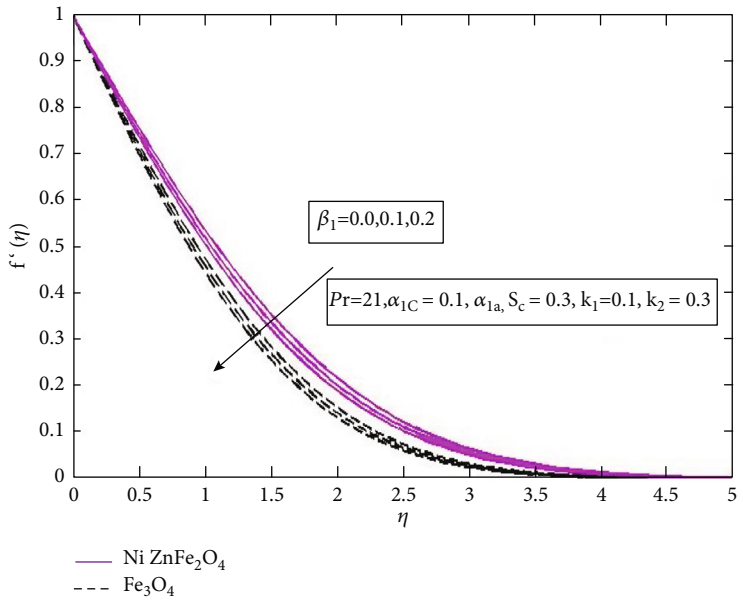

Figure 2: Velocity profile with fluctuation in β_1.

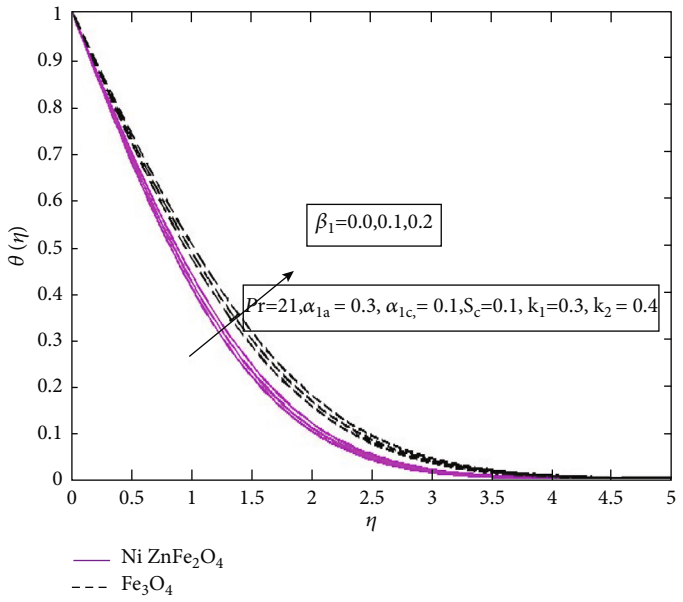

Figure 3: Temperature profile with fluctuation in β_1.

nondimensional thermal relaxation time, S_c the shows Schmidt number, and k_1 and k_2 describe the strength of homogeneous and heterogeneous reaction parameters, which are defined here as

$$\beta_1 = \frac{I_0 \mu_0 K T_c}{\pi \rho l {\mu_0}^2}, \Pr = \frac{\rho c_p \nu}{k}, \alpha_{1a} = \lambda_{1a} u_0 x_{-1}, \alpha_{1c} = \lambda_{1c} u_0 x$$
$$S_c = \frac{\nu_f}{D_A}, k_1 = \frac{k_c a_0^2}{S}, k_2 = \frac{k_s}{D_A}\sqrt{\frac{\nu_f}{S}}. \tag{18}$$

D_A and D_B are equivalent, i.e., $\delta = 1$; then, we can write as

$$g(\eta) + h(\eta) = 1. \tag{19}$$

Utilizing Eqs. (15)-(16), we get the equation as

$$\frac{1}{S_c} g'' + f g' - k_1 g (1-g)^2 = 0. \tag{20}$$

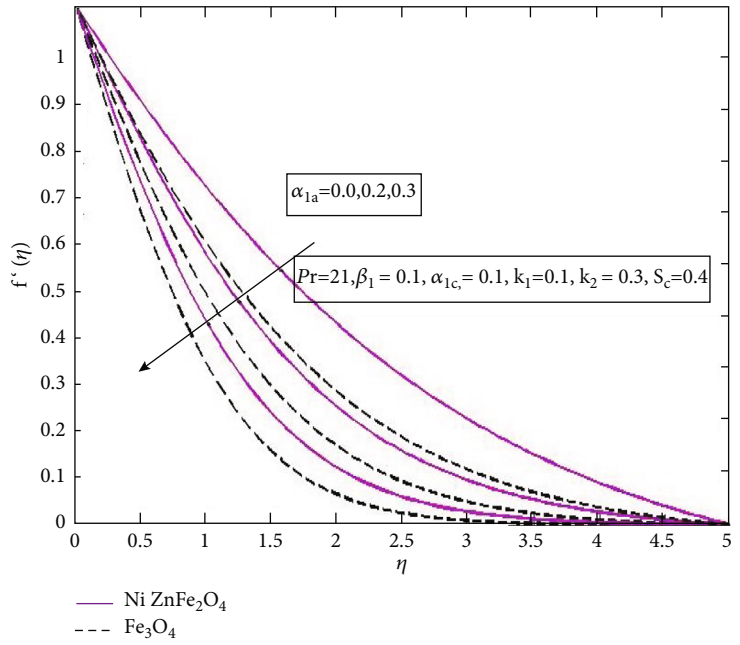

Figure 4: Velocity profile with fluctuation in α_{1a}.

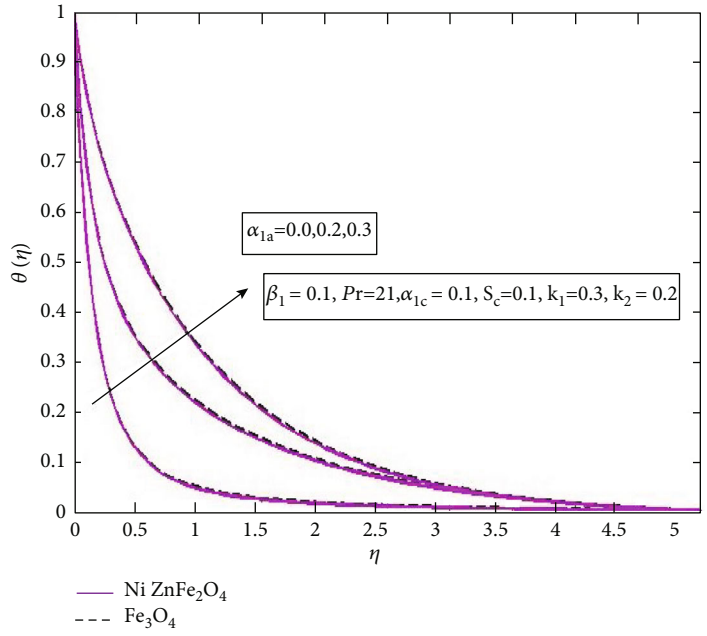

Figure 5: Temperature profile with fluctuation in α_{1a}.

The corresponding boundary equation of the concentration field yields the following form:

$$g'(\eta) = k_2 g(\eta), \eta \longrightarrow 0, g(\eta) = 1, \eta \longrightarrow \infty. \quad (21)$$

The conversions of the wall drag and convective heat transfer into a nondimensional form are scaled as

$$C_f = \frac{-2\tau_w}{\rho_{nf} u_0^2}, Nu = \frac{x k_{nf}}{k_f (T_c - T_w)} \frac{\partial T}{\partial y}\bigg|_{y=0}. \quad (22)$$

The wall shear stress is termed as

$$\tau_w = \mu_{nf} \left(\frac{\partial u}{\partial y}\right)\bigg|_{y=0}, q_w = -k_{nf} \left(\frac{\partial T}{\partial y}\right)\bigg|_{y=0}. \quad (23)$$

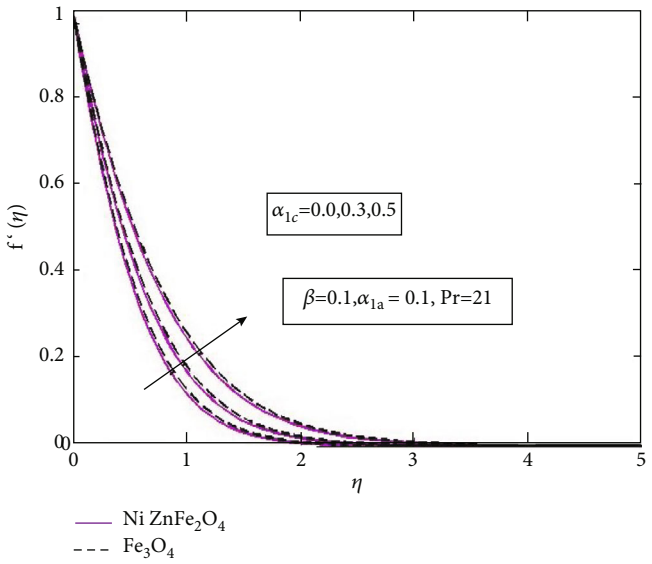

Figure 6: Velocity profile with fluctuation in α_{1c}.

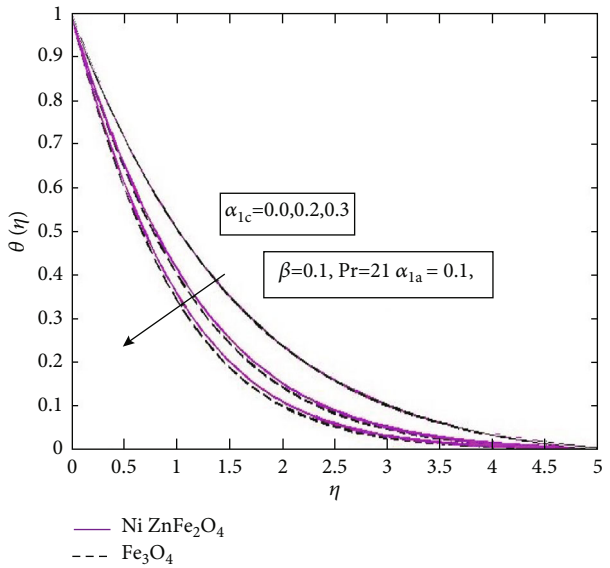

Figure 7: Temperature profile with fluctuation in α_{1c}.

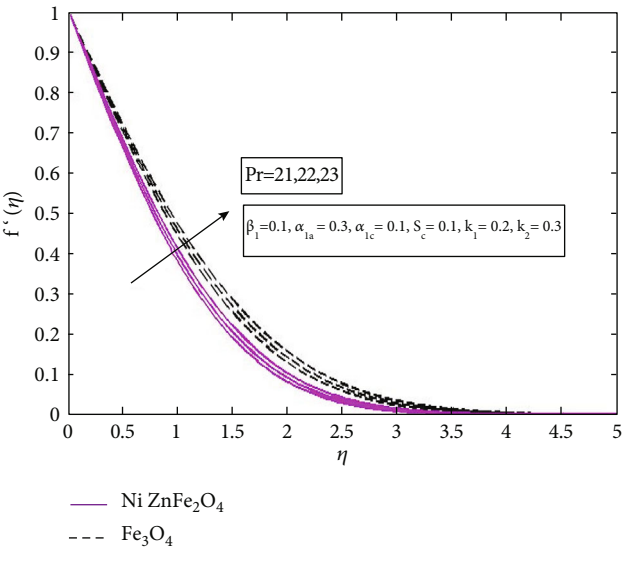

Figure 8: Velocity profile with fluctuation in Pr.

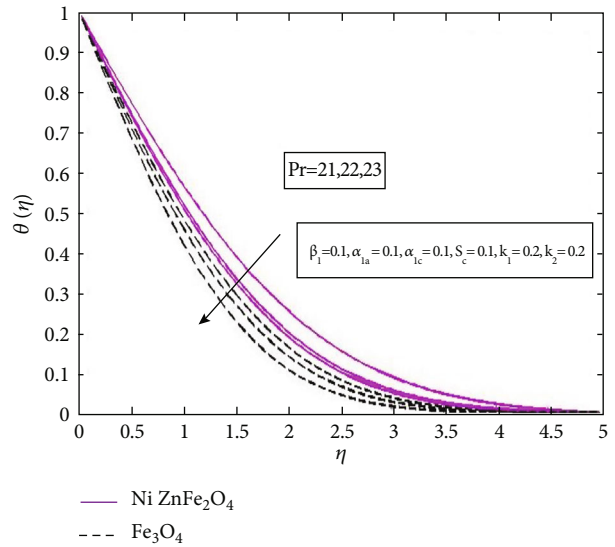

Figure 9: Temperature profile with fluctuation in Pr.

The dimensionless expressions of Eq. (22) are attained:

$$\frac{1}{2}\mathrm{Re}_x^{\frac{1}{2}} C_f = \frac{1}{(1-\phi)^{-2.5}} f''(0), \mathrm{Re}_x^{\frac{-1}{2}} N_{ux} = -\frac{k_{nf}}{k_f}\theta_1'(0), \tag{24}$$

where,

$$\mathrm{Re}_x = \frac{\rho_{nf} u_0 x}{\mu_{nf}}. \tag{25}$$

3. Numerical Methodology

The saturation of two ferrite particles into Maxwell fluid under the action of a double magnetic dipole is examined with homogeneous and heterogeneous reactions. The transformed nonlinear systems of ODEs are solved numerically using the shooting method along with the RK-45 algorithm. For the implementation of the shooting method, one should convert the boundary value problem into an initial value problem. The reduce initial value problem is further converted into a system of first order differential equations and then solved by choosing the missing conditions as an initial guess. Therefore, the suitable transformations are used to obtain initial value problem. The new set of variables for

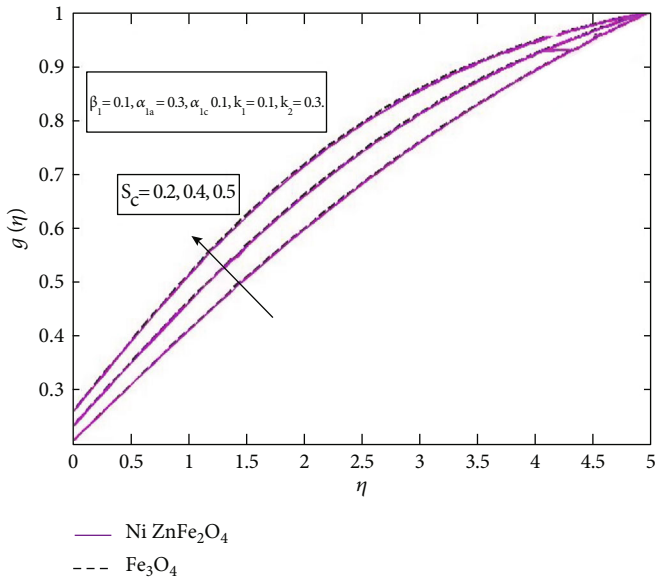

Figure 10: Concentration profile with fluctuation in S_c.

first order system of equations is defined as

$$\left(y_1, y_2, y_3, y_4, y_5, y_6, y_{7=f,f',f'',\theta,\theta',g,g'}\right)'. \tag{26}$$

This substitution yields

$$y_1' = y_2, y_1' = y_2, \tag{27}$$

$$y_2' = y_3, \tag{28}$$

$$y_3' = \left(1/\frac{1}{(1-\phi)^{2.5}\left(1-\phi+\phi\left(\rho_s/\rho_f\right)\right)} - \frac{\alpha_{1a}y_1^2}{4}\right) * \left(-\frac{y_1y_3}{2} + \frac{\alpha_{1a}}{4}\left(y_2^2y_3\eta + 2y_1y_2y_3\right) + \frac{\beta y_4}{\left(1-\phi+\phi\left(\rho_s/\rho_f\right)\right)}\right), \tag{29}$$

$$y_4' = y_5 \tag{30}$$

$$y_5' = \left(1/\frac{k_{nf}/k_f}{1-\phi+\phi^*((\rho Cp)s/(\rho Cp)f)} - \frac{\alpha_{1c}\,\mathrm{Pr}\,f^2}{4}\right) * \left(\mathrm{Pr}^*\left(-\frac{y_1y_5}{2} + y_2y_4 - \frac{\alpha_{1c}}{4}\left(2y_1y_3 + 2y_3y_2y_5\right)\right)\right), \tag{31}$$

$$y_6' = y_7 \tag{32}$$

$$y_6' = -S_c\left(y_1y_7 - k_1\left(y_6\left(1-y^2{}_7\right)^2\right)\right). \tag{33}$$

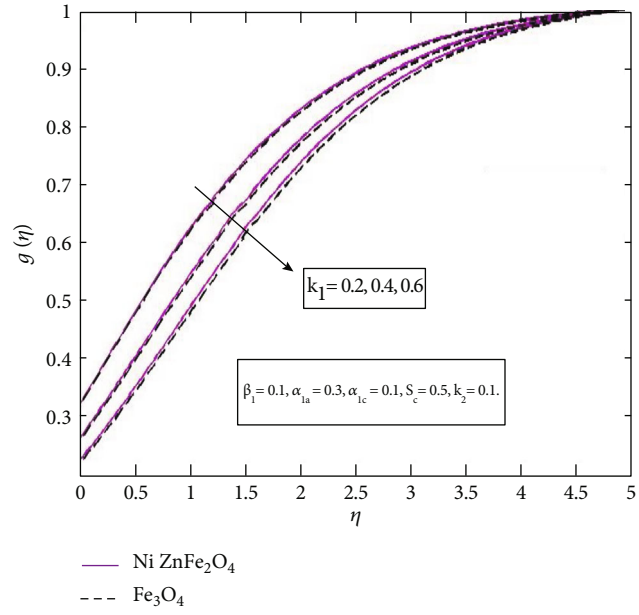

Figure 11: Concentration profile with fluctuation in k_1.

which are subject to the following conditions:

$$y_1(0) = 0, y_2(0) = 0, y_3(0) = \omega_1 \text{ (unknown initial condition)},$$
$$y_4(0) = 1, y_5(0) = \omega_2 \text{ (unknown initial condition)},$$
$$y_7(0) = k_2y_6(0), y_8(0) = \omega_3 \text{ (unknown initial condition)}. \tag{34}$$

To solve the above system of Eqs. (27)-(33), the values of ω_1, ω_2, and ω_3 are unknown, so by taking a suitable initial guess, the convergent numerical solution is obtained. It is important to note that if the boundary residuals are fewer than the tolerance error 10-6, the calculated solution

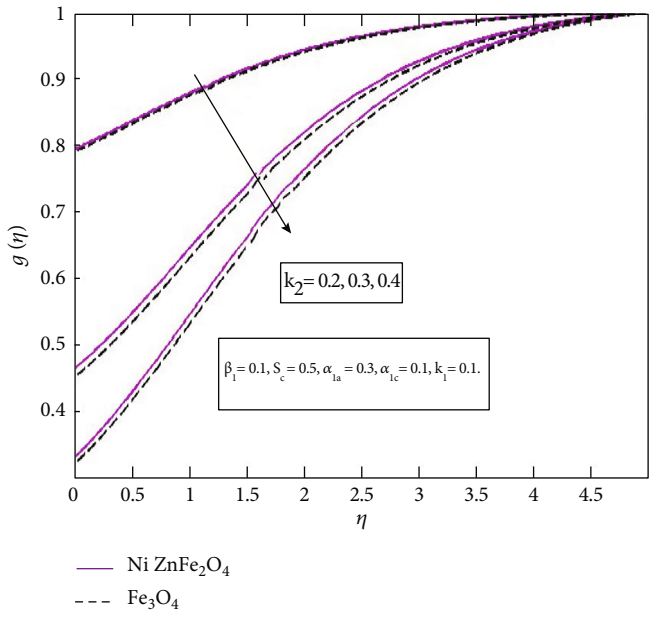

Figure 12: Concentration profile with fluctuation in k_2.

converges. If the computed results do not satisfy this requirement, the initial estimates are changed by using Newton's technique, and the procedure is repeated until the solution fulfills the specified convergence threshold. The thermophysical properties of the base fluid and ferrite particles for numerical procedure are defined in Table 1.

4. Results and Discussion

The mathematical model of chemically reactive viscoelastics fluid over the stretching surface is solved numerically. The numerical solutions are checked by applying the grid independence test. The analysis is performed at different tolerance levels for Nusselt number and skin friction coefficient. The numerical values of Nusselt number and skin friction are presented in Table 2.

Table 3 represents the performance of quantity of engineering interest (Nusselt number) against ferrohydrodynamic interaction (β) and Prandtl number (Pr) in both cases nickel zinc ferrite ($NiZnFe_2O_4$) and magnetite ferrite (Fe_2O_4). It is depicted that the increment occurs in the Nusselt number due to the increasing values ofPr, with better results of magnetite ferrite(Fe_2O_4)as compared to nickel zinc ferrite($NiZnFe_2O_4$). Table 4 displays the response of mass flux coefficient against the strength of homogeneous and heterogeneous parameters and Schmidt number. It is perceived that the mass flux coefficient shows a positive trend towards the strength of homogeneous (k_1) and heterogeneous parameters (k_2) while an opposite behavior seen in the case of the Schmidt number (S_c). The higher magnitude was observed in the case of nickel zinc ferrite.

The analyzation of ferrohydrodynamic interaction (β_1) on velocity field is seen in Figure 2. It is depicted that the velocity decreases due to the increasing values of ferrohydrodynamic interaction parameter (β_1). This opposite behavior is due to the action of Lorentz forces which resist the flow and provide more resistance to transportation phenomena. From the graph, it is cleared that the magnetite ferrite offers more resistance due to which the velocity profile decreases in the case of magnetite ferrite (Fe_3O_4). Figure 3 results an inclination in temperature with altering values of β_1. It is detected that the temperature profile boosts up as soon as the ferrohydrodynamic interaction parameter (β_1) enhances. Reasoned is that Lorentz forces which produces under the action of magnetic field have the potential to produce resistance which in term produce heating among the layers of fluids hence thermal boundary layer thickness rises. It is also perceived that the magnetite ferrite (Fe_3O_4) offers more resistance due to which the rapid temperature enhancement occurred in the case of the magnetite ferrite (Fe_3O_4). The sketch of velocity with augmenting values of Deborah number (α_{1a}) is displayed in Figure 4. It is detected that the increasing Deborah number results in a decreasing velocity profile. As (α_{1a}) precisely relate to relaxation time of fluid, immediately (α_{1a}) increasing fluid relaxation time shot up and provide extra blocking to the fluid motion which results in thinning momentum boundary layer thickness. The maximum velocity is depicted in the case of nickel zinc ferrite ($NiZnFe_2O_4$). The graph of Deborah number (α_{1a}) against the temperature field is seen in Figure 5. It is perceived that the augmented values of the Deborah number (α_{1a}) amplifies the temperature field. This phenomena can be depicted as the enlarging Deborah number (α_{1a}) tends to have a larger relaxation time of fluid which directly means to offer resistance and generates heat which enhances the temperature profile. The effects of the thermal relaxation parameter (α_{1c}) upon the velocity profile is observed in Figure 6. It is clear from the figure that the increasing thermal relaxation parameter (α_{1c}) is responsible for the increasing velocity profile. This fact is explained as by up surging

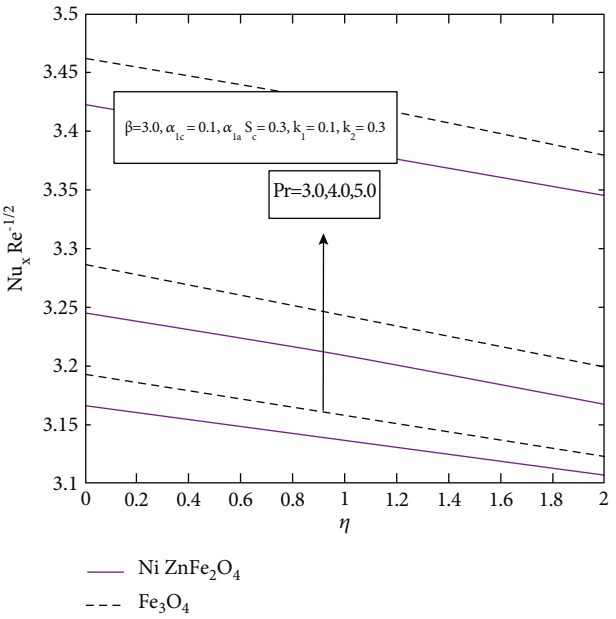

Figure 13: Nusselt number with mutation of β and Pr..

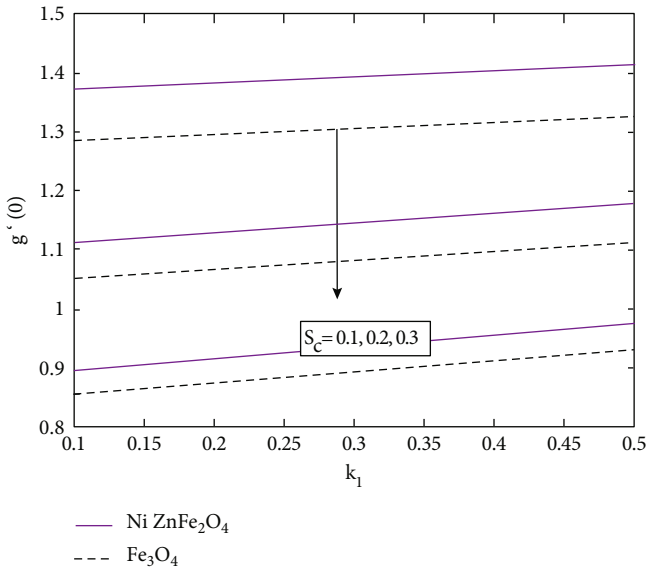

Figure 14: Mass flux coefficient with mutation of k_1 and S_c..

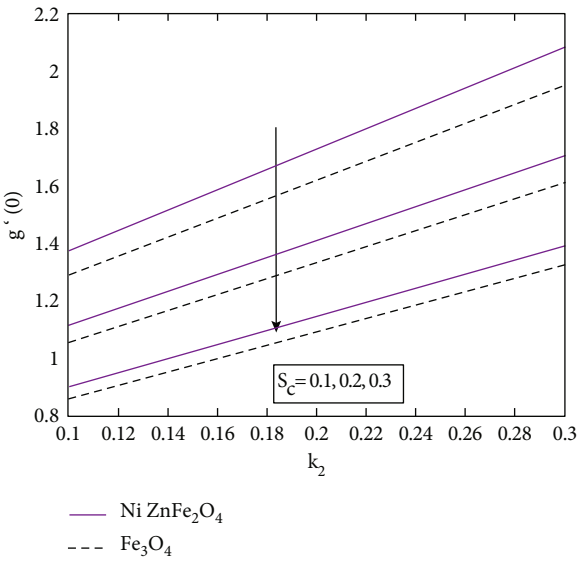

Figure 15: Mass flux coefficient with mutation of k_2 and S_c..

thermal relaxation parameter (α_{1c}) momentum of fluid particles also enhances which in term increase kinetic energy and velocity profile. Figure 7 enlightened the conduct of thermal relaxation time (α_{1c}) on the temperature field. By expanding values of (α_{1c}) temperature profile show reverse behavior, because enlarging thermal relaxation time implies materials particles demand extra pace to exchanging energy to their connecting particles, thus cause reduction in temperature profile. The impression of Prandtl number on velocity is realized in Figure 8. The increasing behavior of velocity is observed by the altering values of the Prandtl number, which is due to straight forward relation between the Prandtl number and momentum diffusivity. As soon as the Prandtl increases, the momentum diffusivity also increases; thus, in the result, fluid motion and momentum boundary layer thickness also boost up. Association between Prandtl number and temperature field clearly delineated in Figure 9, the contrary response of temperature towards Prandtl number, actually Prandtl number exhibit inverse relation to thermal diffusivity of fluid, So by enhancing Prandtl number directly means to lessen diffused heat betwixt fluid layers hence reduces temperature profile. The response of Schmidt number (S_c) towards the concentration field is characterized in Figure 10. The increase in Schmidt number (S_c) consequently increases the concentration field because the concentration field relates with a viscous diffusion rate to molecular diffusion rate, so when the Schmidt number (S_c) magnifies the viscous diffusion rate, it also magnifies which in turn enhances the concentration field. Figure 11 shows the connection between the strength of homogeneous reaction parameter (k_1) and concentration field. It is observed by enhancing the strength of homogeneous parameter(k_1)concentration field that is going to shrink. This conduct is explained as reactants are consumed during the process of homogeneous reaction which depresses concentration profile. Also, the minimum concentration was observed in case of magnetite ferrite (Fe_3O_4). The graph of concentration field against the altering values of strength of heterogeneous reaction parameter (k_2) is displayed in Figure 12. An increase in (k_2) causes a reduction in concentration field, while higher concentration is found in the case of nickel zinc ferrite ($NiZnFe_2O_4$). Figure 13 shows the impact of Pr number upon a heat transfer rate. As we increase the Prandtl number, the Nusselt number also increases because by increasing Prandtl number rate of momentum, the diffusivity also increases which gives rise to the kinetic energy and also the heat transfer through convection. The impact of strength of homogeneous parameter (k_1) and Schmidt number (S_c) in the mass flux coefficient

$g'(0)$ is carried out in Figure 14. It is seen that (S_c) shows a negative response, while (k_1) displays an augmented amplitude against $(g'(0))$. Figure 15 depicts the trend of $(g'(0))$ that relates with the strength of the heterogeneous parameter and Schmidt number (S_c). As it is remarked because of the amplification in (k_2), the mass flux coefficient $(g'(0))$ magnifies due to the accumulation of particles by the generation of the heterogeneous mixture. Also in the case of (S_c), we observed that as soon as (S_c) increases, the Sherwood number $(g'(0))$ reduces by reducing the mass diffusivity.

5. Concluding Remarks

In this article, we have examined the response of double magnetic dipole in a chemically reactive viscoelastic fluid over a flat sheet by considering the two nanomagnetic ferrite particles. For heat transfer rate, we used the Cattaneo-Christov heat flux model which is the generalization of Fourier law by including thermal relaxation term. The thermal relaxation time converts the energy transport in form of thermal waves with finite speed. The modeled PDEs are converted into the system of ODEs and then solved numerically by shooting method. The results are depicted graphically with the impact of important parameters. The major outcomes of this study are as follows:

(i) Due to the force generated by magnetic dipoles, the velocity of the fluid reduces, and the temperature increases by increasing the ferrohydrodynamic interaction parameter β_1

(ii) For the large value of Deborah number (α_{1a}), the velocity profile decreases

(iii) The thermal relaxation parameter (α_{1c}) shows a positive response towards velocity while the negative response towards temperature because particles take a surplus time to shifting energy

(iv) The strength of homogeneous reaction parameter k_1 undermines concentration

(v) The concentration field depresses due to the presence of strength of heterogeneous reaction parameter k_2

(vi) It has been observed that heat transfer rate increases in the presence of magnetite ferrite ($NiZnFe_2O_4$) as compared to nickel zinc ferrite ($NiZnFe_2O_4$) by increasing Pr

(vii) From physical point of view, Pr is the proportion of momentum diffusivity to thermal diffusivity. The contrary response of temperature towards the Prandtl number is observed; actually, the Prandtl number exhibits an inverse relation to thermal diffusivity of the fluid, so by enhancing Prandtl number directly means to lessen the diffused heat between fluid layers and hence reduce the temperature profile

Nomenclature

u, v: Velocity components
l: Length of plate
T_w: Surface temperature
T_c: Curie temperature
μ_0: Magnetic permeability
μ_{nf}: Dynamic viscosity of nanofluid
μ_f: Dynamic viscosity of base fluid
k_{nf}: Thermal conductivity of nanofluid
ρ_{nf}: Density of nanofluid
$(\rho c_p)_f$: Heat capacitance of fluid
$(\rho c_p)_s$: Heat capacitance of solid particle
$(\rho c_p)_{nf}$: Heat capacitance of nanofluid
H_x: Magnetic field intensity along x direction
H_y: Magnetic field intensity along y direction
M: Magnetization
υ: Kinematic viscosity
τ_w: Wall shear stress
λ_{1a}: Relaxation time of fluid
λ_{1c}: Relaxation time of heat flux
α_{1a}: Deborah number in case of double dipole
α_{1c}: Thermal relaxation in case of double dipole
S_c: Schmidt number
k_1: Strength of homogeneous reaction
k_2: Strength of heterogeneous reaction
ζ: Tolerance rate
δ: Ratio of mass diffusion coefficients
δ_a: Magnetic scalar potential.

Data Availability

Data are available within the article.

Conflicts of Interest

The authors declare no conflict of interest.

Acknowledgments

This study is supported by the Taif University Researchers Supporting Project number (TURSP-2020/31), Taif University, Taif, Saud Arabia.

References

[1] S. S. Papell, *United States Patent Office Filed Ser*, 1963.

[2] M. A. Chaudhary and J. H. Merkin, "A simple isothermal model for homogeneous-heterogeneous reactions in boundary-layer flow.II Different diffusivities for reactant and autocatalyst," *Fluid Dynamics Research*, vol. 16, no. 6, pp. 335–359, 1995.

[3] J. H. Merkin, "A model for isothermal homogeneous-heterogeneous reactions in boundary-layer flow," *Mathematical and Computer Modelling*, vol. 24, no. 8, pp. 125–136, 1996.

[4] H. I. Andersson and O. A. Valnes, "Flow of a heated ferrofluid over a stretching sheet in the presence of a magnetic dipole," *Acta Mechanica*, vol. 128, no. 1-2, pp. 39–47, 1998.

[5] R. Ganguly, S. Sen, and I. K. Puri, "Heat transfer augmentation using a magnetic fluid under the influence of a line dipole," *Journal of Magnetism and Magnetic Materials*, vol. 271, no. 1, pp. 63–73, 2004.

[6] A. Sharma, D. Sharma, and R. C. Sharma, "Effect of dust particles on thermal convection in a ferromagnetic fluid," *Zeitschrift für Naturforschung A*, vol. 60, pp. 7494–7502, 2005.

[7] T. Strek, "Heat Transfer in Ferrofluid in Channel with Porous Walls," in *Proceedings of the COMSOL Users Conference*, pp. 1–12, Prague, Czech Republic, 2006.

[8] T. Strek and H. Jopek, "Computer simulation of heat transfer through a ferrofluid," *Physica status solidi*, vol. 244, no. 3, pp. 1027–1037, 2007.

[9] M. A. Sadiq and H. M. S. Bahaidarah, "Numerical study on generalized heat and mass in Casson fluid with hybrid nanostructures," *Journal of Nanometers*, vol. 11, no. 10, p. 2675, 2021.

[10] O. D. Makinde and A. Aziz, "Boundary layer flow of nanofluid past a stretching sheet with a convective boundary condition," *International Journal of Thermal Sciences*, vol. 50, no. 7, pp. 1326–1332, 2011.

[11] H. Aminfar, M. Mohammadpourfard, Y. Narmani Kahnamouei, M. M. Pourfard, and Y. N. Kahnamouei, "A3D numerical simulation of mixed convection of a magnetic nanofluid in the presence of non-uniform magnetic field in a vertical tube using two phase mixture model," *Journal of Magnetism and Magnetic Materials*, vol. 323, no. 15, pp. 1963–1972, 2011.

[12] N. Bachok, A. Ishak, and I. Pop, "On the stagnation-point flow towards a stretching sheet with homogeneous-heterogeneous reactions effects," *Communications in Nonlinear Science and Numerical Simulation*, vol. 16, no. 11, pp. 4296–4302, 2011.

[13] H. Aminfar, M. M. Pourfard, and S. A. Zonouzi, "Numerical study of the ferrofluid flow and heat transfer through a rectangular duct in the presence of anon-uniform transverse magnetic field," *Journal of Magnetism and Magnetic Materials*, vol. 327, pp. 31–42, 2013.

[14] P. K. Kameswaran, S. Shaw, P. Sibanda, and P. V. S. N. Murthy, "Homogeneous-heterogeneous reactions in a nanofluid flow due to porous stretching sheet," *International Journal of Heat and Mass Transfer*, vol. 57, no. 2, pp. 465–472, 2013.

[15] L. S. R. Titus and A. Abraham, "Heat transfer in ferrofluid flow over a stretching sheet with radiation," *International Journal of Engineering Research & Technology*, vol. 3, 2014.

[16] M. Sheikholeslami, M. M. Rashidi, and D. D. Ganji, "Effect of non-uniform magnetic field on forced convection heat transfer of Fe3O4-water nanofluid," *Computer Methods in Applied Mechanics and Engineering*, vol. 294, pp. 299–312, 2015.

[17] T. Hayat, M. Imtiaz, and A. Alsaedi, "MHD flow of nanofluid with homogeneous-heterogeneous reactions and velocity slip," *Thermal Science*, vol. 67, 2015.

[18] M. Imtiaz, T. Hayat, A. Alsaedi, and A. Hobiny, "Homogeneous-heterogeneous reactions in MHD flow due to an unsteady curved stretching surface," *Journal of Molecular Liquids*, vol. 221, pp. 245–253, 2016.

[19] A. Majeed, A. Zeeshan, and R. Ellahi, "Unsteady ferromagnetic liquid flow and heat transfer analysis over a stretching sheet with the effect of dipole and prescribed heat flux," *Journal of Molecular Liquids*, vol. 223, pp. 528–533, 2016.

[20] T. Hayat, M. Waqas, S. A. Shehzad, and A. Alsaedi, "On 2D stratified flow of an Oldroyd-B fluid with chemical reaction: an application of non-Fourier heat flux theory," *Journal of Molecular Liquids*, vol. 223, pp. 566–571, 2016.

[21] T. Hayat, M. I. Khan, M. Farooq, A. Alsaedi, M. Waqas, and T. Yasmeen, "Impact of Cattaneo-Christov heat flux model in flow of variable thermal conductivity fluid over a variable thicked surface," *International Journal of Heat and Mass Transfer*, vol. 99, pp. 702–710, 2016.

[22] M. Sajid, S. A. Iqbal, M. Naveed, and Z. Abbas, "Effect of homogeneous-heterogeneous reactions and magnetohydrodynamics on Fe_3O_4 nanofluid for the Blasius flow with thermal radiations," *Journal of Molecular Liquids*, vol. 233, pp. 115–121, 2017.

[23] S. U. Rehman, A. Zeeshan, A. Majeed, and M. B. Arain, "Impact of Cattaneo-Christov heat flux model on the flow of Maxwell ferromagnetic liquid along a cold flat plate embedded with two equal magnetic dipoles," *Journal of Magnetic*, vol. 22, no. 3, pp. 472–477, 2017.

[24] U. Nazir, M. A. Sadiq, and M. Nawaz, "Non-Fourier thermal and, mass transport in hybrid nano-Williamson fluid under chemical reaction in Forchheimer porous medium," *International Communication in Heat and Mass Transfer*, vol. 127, article 105536, 2021.

[25] M. A. Qureshi, S. Hussain, and M. A. Sadiq, "Numerical simulation of MHD mixed convection of hybrid nano fluid flow in a horizontal channel with cavity impact on heat transfer and hydro nano forces," *Journal of Case Studies in Thermal Engineering*, vol. 27, article 101321, 2021.

[26] W. Tahir, S. Bilal, N. Kousar, I. A. Shah, and A. S. Alqahtani, "Analysis about enhancement in thermal characteristics of viscous fluid flow with induction of ferrite particles by using cattaneo christov theory," *Proceedings of the Institution of Mechanical Engineers, Part C: Journal of Mechanical Engineering Science*, vol. 236, no. 1, pp. 208–218, 2022.

[27] M. A. Sadiq, "Non-Fourier heat transfer enhancement in Power law fluid with mono and hybrid nano particles," *Journal in Research Square*, vol. 11, 2021.

[28] M. A. Sadiq, "Heat transfer of a nanoliquid thin film over a stretching sheet with surface temperature and internal heat generation," *Journal of Thermal Analysis and Calorimetry*, vol. 143, no. 3, pp. 2075–2083, 2021.

[29] A. Saeed, P. Kumam, T. Gul, W. Alghamdi, W. Kumam, and A. Khan, "Darcy–Forchheimer couple stress hybrid nanofluids flow with variable fluid properties," *Scientific Reports*, vol. 11, no. 1, pp. 1–13, 2021.

[30] T. Gul, M. Rehman, A. Saeed et al., "Magnetohydrodynamic impact on Carreau thin film couple stress nanofluid flow over an unsteady stretching sheet," *Mathematical Problems in Engineering*, vol. 2021, 10 pages, 2021.

[31] A. Saeed, P. Kumam, S. Nasir, T. Gul, and W. Kumam, "Nonlinear convective flow of the thin film nanofluid over an inclined stretching surface," *Scientific Reports*, vol. 11, no. 1, pp. 1–15, 2021.

[32] M. Bilal, A. Saeed, T. Gul, I. Ali, W. Kumam, and P. Kumam, "Numerical approximation of microorganisms hybrid nanofluid flow induced by a wavy fluctuating spinning disc," *Coatings*, vol. 11, no. 9, p. 1032, 2021.

[33] T. Gul, M. Usman, I. Khan et al., "Magneto hydrodynamic and dissipated nanofluid flow over an unsteady turning disk," *Advances in Mechanical Engineering*, vol. 13, no. 7, 2021.

[34] A. Rehman, Z. Salleh, and T. Gul, "Heat transfer of thin film flow over an unsteady stretching sheet with dynamic viscosity," *Journal of Advanced Research in Fluid Mechanics and Thermal Sciences*, vol. 81, no. 2, pp. 67–81, 2021.